ISSN 2409–4951(Online)
ISSN 2310–1008 (Print)

Ukrainian Journal of Food Science

Volume 8, Issue 1
2020

Kyiv 2020

Comprehensive analysis of innovative devices based on shape memory alloys in food technology apparatuses

Anatoliy Ukrayinets, Volodymyr Shesterenko, Volodymyr Romaniuk

National University of Food Technologies, Kyiv, Ukraine

Keywords:

Apparatus
Temperature
Shape
Memory
Thermal drive
Thermal valve
Heliodrive

Article history:

Received 30.11.2019
Received in revised form 26.03.2020
Accepted 30.06.2020

Corresponding author:

Volodymyr Shesterenko
E-mail:
shest.iren.co@ukr.net

DOI: 10.24263/2310-1008-2020-8-1-12

Abstract

Introduction. The purpose of this study is to conduct a comprehensive analysis of innovative devices based on shape memory alloys (SMA's) for use in food technology apparatuses.

Materials and methods. Physical and mathematical processes modeling, principles of the theory of automatic control, the theory of fuzzy logic were used.

Results and discussion. The complex analysis of devices based on materials with shape memory effect (SME), which can be applied to food industry apparatuses, is made. In particular, design and principle of operation of the thermal valves, characterized by simplicity of construction and reliability, were analyzed. Design and principle of operation of the critical temperature increase indicator for machine's casing and the nut-indicator for overheating of sectional casing of technological machine, which increase the reliability of apparatuses were analized. Design and principle of operation of the thermal drives which can be effectively used in factories that need to utilize low-temperature thermal energy were analized. Design and principle of operation of the heliodrive were analized.

Design of the critical temperature increase indicator for machine's casing is highly technological and reliable.

Many factories need to utilize heat energy at relatively low temperature difference. These requirements are met by the design of the thermal drive.

Power elements based on SME alloys have significant advantages: less mass, they can work in a wide temperature range, they have small dimensions, smooth movement of working parts, lower cost, high sensitivity.

Drives based on heat-sensitive elements with SME are effective in solar power installations.

Introduction

SME materials can be used in food industry to optimize the operation of its apparatuses (improving their reliability, preventing their failure, recycling secondary energy, etc.) [1-3].

Among the Ukrainian developments on this topic the thermal valves, the critical temperature increase indicator for machine's casing, semaphore-light indicator of heating of current-carrying elements and contact connections of technological apparatus can be mentioned (patent of Ukraine №17994, F03G 7/06./Ukrayinets A.I. Shesterenko V.Ye., patent of Ukraine №19634/Ukrayinets A.I. Shesterenko V.Ye., patent of Ukraine № 42169, H01R 11/00. /Ukrayinets A.I. Shesterenko V.Ye.). Among the foreign developments, similar in function to the overheating indicator is, for example, Temperature-sensitive indicator nut (Chinese patent CN105157861A).

The problem is that these developments are not widespread and described in detail. There are some researches devoted to use of SME materials as actuators [4-17], but not in food industry. To understand the advantages or disadvantages of using SME materials in devices to improve the efficiency of food industry apparatuses, the task of analyzing these devices is urgent.

Thus, the purpose of this study is to conduct a comprehensive analysis of innovative devices based on shape memory alloys (SMA's) for use in food technology apparatuses.

Materials and methods.

Two Cu–Al–Ni alloys containing 15% Al, 9% Ni (alloy I) and 14% Al, 5% Ni (alloy II) were taken for the study. The alloys were quenched from 900°C in NaOH solution. The grain size of the β phase is 0,3–0,6 mm. Phase composition of the alloys after quenching was determined by X-ray imaging, and the temperature intervals β_1–γ^1 of the transformation were determined along the curves of change of electrical resistance during heating and cooling. The martensitic point of the alloy I is +10°C, for the alloy II it is +110°C. Samples of size 2,0x0,7x40mm were loaded according to the scheme of four-point bending and by the curve of the section loaded with constant bending moment, the radius of curvature was found (deflection was determined to within 0,02 mm). The research was conducted on equipment of NAS of Ukraine.

Deformation is determined by the radius of curvature, assuming that after deformation cross section remains flat. Maximal stresses in the samples deformed above A_f were determined taking into account deviation of dependence between stress and deformation from the Hooke's law [18], and it was considered that the deformations in the compressed and stretched sections of the beam (sample) were equal. This assumption is justified by the fact that deviation from the Hooke's law in this case is caused by the martensitic transformation. The samples were loaded under isothermal conditions in temperature range from –196°C to +200°C.

Elastic properties of the taken bronze change significantly with temperature.

As long as applied load is insufficient to cause formation of martensitic crystals at given temperature, the dependence of $\delta(\varepsilon)$ is linear.

The beginning of deviation from this linear dependence coincides with the appearance of the martensitic phase in the sample.

An X-ray analysis confirmed that the sample of the alloy I bent at room temperature contained a significant amount of the martensitic phase.

When unloaded, the martensite crystals disappear with a certain hysteresis and, if the deformation was carried out at a temperature above +20°C (temperature A_f for the alloy I),

the sample completely restores its original shape. Above 150°C, the dependence of $\delta(\varepsilon)$ is linear. In the temperature range of 20–150°C, stress at which the martensitic deformation mechanism begins to act increases linearly with temperature.

Thermal effect of the transformation was determined by change in heat capacity of the alloy II with high-speed heating. In the temperature range of the reverse transformation there is a sharp decrease in heat capacity associated with emission of latent heat of the transformation. If at some temperature higher than A_f we load the sample in such a way that it causes appearance of the martensitic phase and then (without removing the load) heat it, the deformation will change. As the temperature rises, martensite gradually disappears, leading to the deformation (restoration of the initial shape) of the sample.

After deformation in the temperature range below A_f, the unloading does not end with complete restoration of the form (shape). The original shape is restored only when heated as a result of the reverse martensitic transformation. If deformation is carried out at a temperature below the martensitic point (M_s), then to obtain a certain degree of final deformation the higher loads are required at the lower temperatures.

The small hysteresis between the loading and unloading curves can be explained by the elastic twinning in martensite observed in these alloys experimentally [19-21].

It should be noted that in all cases of deformation below A_f, the samples while retaining the final deformation after unloading, restored their original shape after heating.

Since the main cause of the stop of crystal growth during martensitic transformation is the accumulation of elastic energy, it is of interest to estimate the possible level of stresses arising in the material during martensitic rearrangement. The change in thermodynamic potential caused by the growing crystal of martensite is expressed as follows:

$$\Delta W = -\Delta\Phi + S_\gamma + E, \quad (1)$$

where $\Delta\Phi$ – chemical thermodynamic driving force of transformation, S_γ – surface energy at the interface, E – elastic energy.

$$\frac{dT_0}{d\delta} = \frac{1}{\rho} = \frac{T_0 \cdot \varepsilon}{\Delta H \cdot A}, \quad (2)$$

where T_0 – thermodynamic equilibrium temperature, δ – external stress, ε – transformation deformation (ε=0,11), ρ – density, ΔH – thermal effect of transformation, A – mechanical equivalent of heat.

The authors manufactured thermomechanical converters with SME made of aluminum bronze Cu–Al–Ni (12÷16% Al; 0÷10% Ni). The elements (D_{out}=5 mm; d_{in}≈3 mm; l=4 mm; t=1,5 mm; s=0,7 mm) had the form of a coiled spring with a rectangular cross-section of the coil. They were examined on a special stand, which allows to measure the load on the element, its temperature and deformation. The elements were cooled in vapor of boiling liquid nitrogen at an average rate of 10°K/s. Measurement techniques, sensors and secondary devices provided a maximum standard deviation of $\bar{\sigma} \leq 1.5\%$. The experiment determined the effect of temperature and loading conditions on magnitude of output signal of the elements and force created by them.

On Figure 1 there is typical characteristic of deformation of an element with its change in temperature for specific example presented. Temperatures of the beginning and the end of the direct martensitic transformation accordingly M_s=108,5°K; M_f=93°K and temperatures of the beginning and the end of the reverse martensitic transformation accordingly A_s=115°K; A_f=125,5°K.

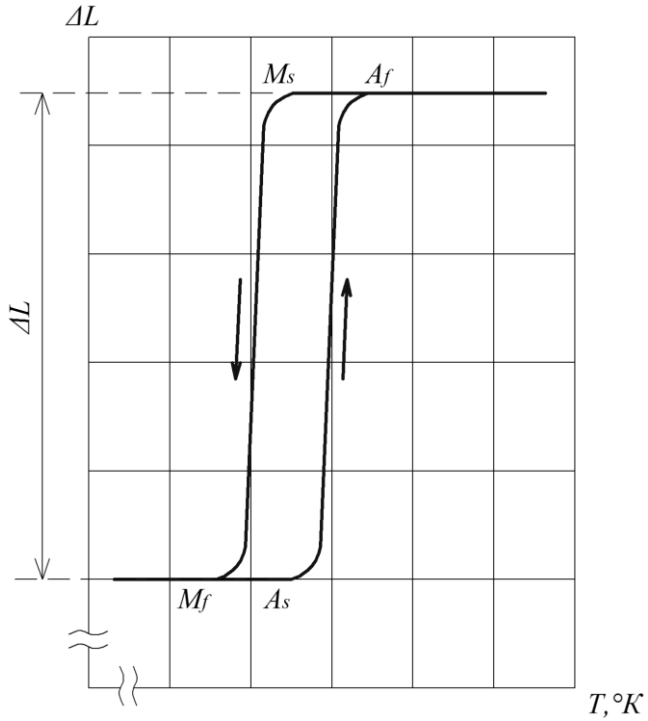

Figure 1. Phase transformations

To clearly show the adwantages of the new thermo-mechanical drives on Figure 2 values of relative temperature deformations $\varepsilon_t = \frac{l_t - l_0}{l_0} = M(T)$ of the elements that are made of Cu-Al-Ni alloy (right scale – experimental dependence) and brass, plastic (left scale – theoretical dependence) are given.

Comparison of curves shows that in the range of operating temperatures 290°–320°K, the sensitivity of an element with SME is greater than other samples in 200–400 times. Calculation of sensitivity:

$$x = \varepsilon_t \frac{l_0}{\Delta T} \tag{3}$$

It is found that the value of triggering temperature of the elements (beginning of the direct – M_s and the reverse – A_s transformations) is changing with the load (Figure 3) [2].

This means that by varying the load on the element, the working point of the element shifts. It is important to take this fact into account while designing and making calculations of the devices that are based on the elements with SME.

The equasion for the coefficient of the energy transition in an element with SME:

$$\eta_{n.ф.} = \frac{\Delta H}{c'_m} \frac{\ln(1+\frac{\Delta T_{ф.n.}}{T})}{\frac{\Delta T_{ф.n.}}{T}(T - T_{o.c.})}, \tag{4}$$

where c'_m – averaged thermal capacity of an element in temperature range of the phase transformation $\Delta T_{ф.n.} = A_f - A_s$.

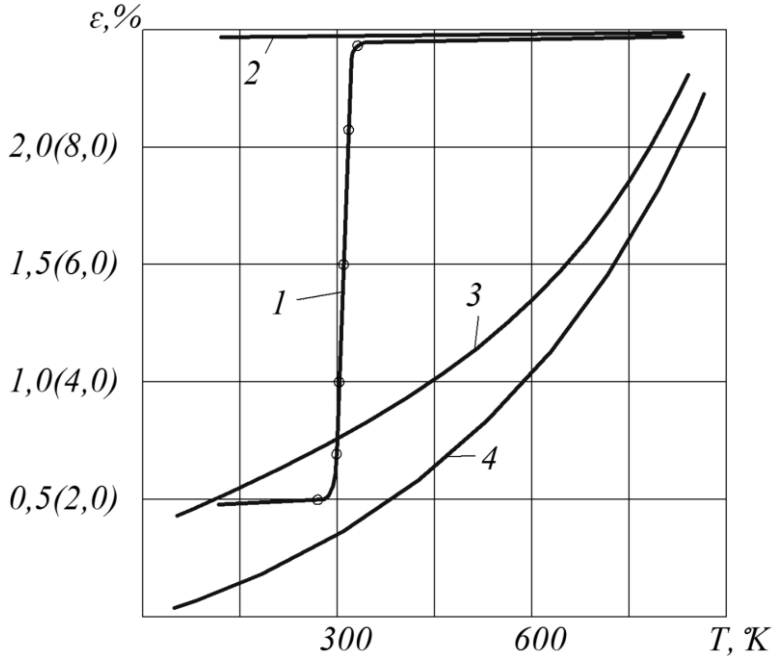

Figure 2. Relative temperature deformations of thermosensitive elements made of materials: 1 – SMA (deformation in brackets); 2 – brass; 3 – teflon (PTFE); 4 – polyethylene (PE).

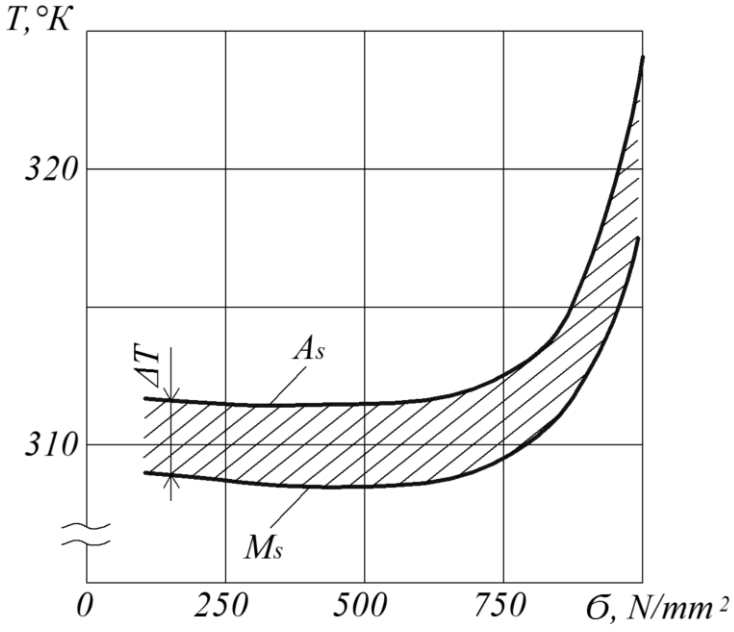

Figure 3. Dependance of SMA triggering temeratures from applied load

Force that is created by the element:

$$P_t = \sigma_\gamma Q, \quad (5)$$

where σ_γ – tension that is generated during the process of shape restoration.

$$\sigma_\gamma = \frac{\Delta H \rho}{\varepsilon_t} \ln \frac{A_f}{A_s}, \quad (6)$$

where ΔH – thermal effect of phase transition for Cu-Al-Ni alloy that was calculated out of the change in themal capacity, equals $8{,}5 \cdot 10^3$ J/kg; ρ – density; ε_t – value of relative deformation.

The calculation for the specific element using equation (4) (T=115 °K and $\Delta T_{ф.п.}$=10 °K) returns $\eta_{п.ф.}$=13%. It is higher by a degree than η of dilatometric converter. After calculation of σ_γ using (5) we get for our example P_t=50 H.

Therefore elements with SME have high sensitivity and can create forces that can be compared with forces that are created by dilatometric converters.

The temperature of phase transformation and form of hysteresis is determined by the composition of the alloys and their heat treatment. Also SMA's are characterized by high strength and manufacturability [2, 4, 19-21].

Results and discussion

Elements made from SME materials are characterized by high sensitivity.

If these materials are used in the manufacture of valves and other regulating equipment they can significantly simplify food production.

Analysis of design and operation of thermal valves based on the SME elements.

Figure 4a shows the construction of the thermal valve. By changing the alloys composition, we can achieve any triggering point in a wide range from –110°C to +600°C. Therefore, when the temperature of the medium flowing through the valve and heating the power element made of SMA rises, the power element, due to the appearance of elastic forces, restores its original shape and closes the pipeline. When the temperature decreases, the power element becomes plastic and under the action of the medium (liquid in the pipeline) opens the pipeline.

The advantages of this valve are its constant readiness to work due to the heating of the flowing fluid, and small energy requirement.

The second type of valve is shown on Figure 4b. This is a thermal-electric valve. In the initial state the valve is closed and held at the saddle with a spring 5, which is simultaneously a directed load of the drive 6, made in the form of a spring made of SME material. To open the valve, the heat source (spiral 7) needs to be turned on. When heated, the actuator 6 increases its linear dimensions, compressing the spring 5 with the help of a rod 3, and the valve 2 opens. The liquid flows through the pipe 1 and the cavity 4 [2].

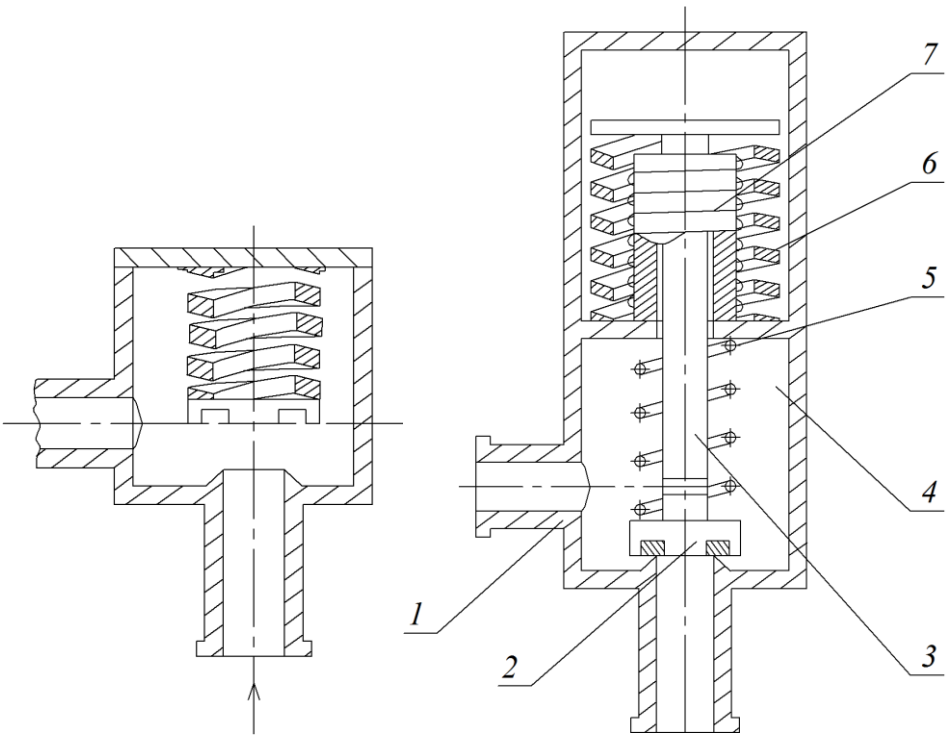

Figure 4. Thermal valves with SME elements used as drives
a – energy source – liquid; b – energy source – electrical current.

Analysis of design and operation of critical temperature increase indicator for machine′s casing

Technical essence of the proposed indicating device is explained by Figure 5.

The temperature of reverse martensitic transformation of the material with SME is equal to the maximum permissible temperature of the machine. When the normal mode of operation of the machine is violated, its temperature starts to rise. Bolt 1 is a heat conductor and it heats the spring 7 that is made of the material with SME. Upon reaching the temperature of reverse martensitic transformation, the spring material 7 rapidly changes its characteristics and tries to restore its original form. The spring 7 substantially increases its length and pushes the cylinder out of the ring groove 5 outwards. The bright fluorescent coating of the outer surface of cylinder 6 allows the staff to respond quickly to the damage. After the temperature of the machine decreases, the material with SME loses its elastic properties, but does not return in the initial position by itself. This is a significant advantage of the device, because the fault of the equipment operating in automatic mode is detected by the staff during maintenance work. The return of the cylinder 6 to the groove 5 is carried out manually during the repair work.

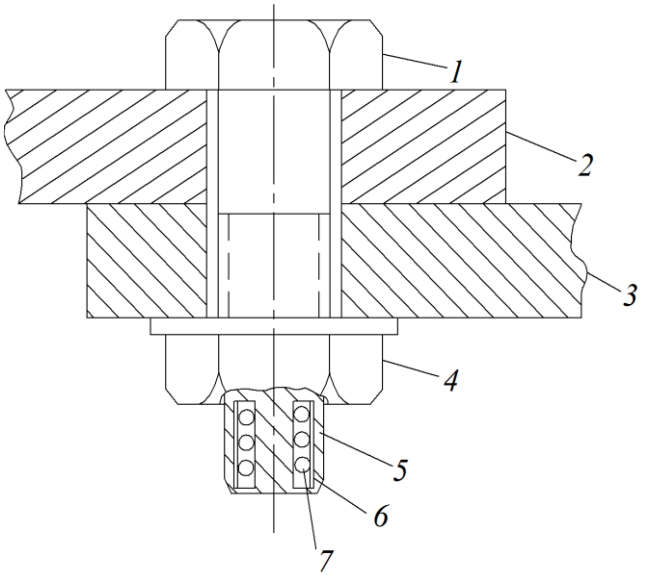

Figure 5. Critical temperature increase indicator for machine's casing in assembled state
Here: 1 – bolt that connects the elements of the casing of the machine 2 and 3, 4 – nut, 5 – ring groove in the tail part of the bolt, 6 – cylinder with surface that has bright fluorescent coating, 7 – cylindrical spring made of the material with SME, one end of the spring 7 is fixed to the bottom of the groove 5, another end is fixed to the cylinder 6.

Analysis of design and operation of nut-indicator for overheating of sectional casing of technological machine

Nut-indicator for overheating of sectional casing of technological machine that would work with high degree of reliability can be created using SME material. The elements of the critical temperature indicator can be made of this material. The technical essence of the proposed indicating device is explained by the Figure 6.

The temperature of reverse martensitic transformation of the material with SME is equal to the maximum permissible temperature of the machine. When the normal mode of operation of the machine is violated, its temperature starts to rise. The bolt 8 is a heat conductor and it heats the washer 7 that is made of the SME material. When the temperature reaches the starting point of reverse martensitic transformation, the washer 7 rapidly changes its characteristics and tries to acquire the shape which it had during its manufacture. Washer 7 bends, increases its height substantially and pushes the flag 6 out of the shank 2, the flag 6 removes the protective cap 3 from the shank 2 of the nut 1. The magnet 4 located on the cap 3 moves relative to the reed switch 5 causing a change in the position of the contacts of the reed switch 5. This sends a signal to the alarm system of technological machine. Fluorescent coating of the outer surface of the flag 6 allows service staff to quickly locate the place of damage of technological machine. After the temperature of the device decreases, the material with SME loses its elastic properties, but does not return to the starting position by itself. This is a significant advantage of the device, because the failure of the equipment operating in automatic mode can be noticed by service staff during maintenance work. Returning of the flag 6 to the shank of the nut 1 is carried out manually during repair work.

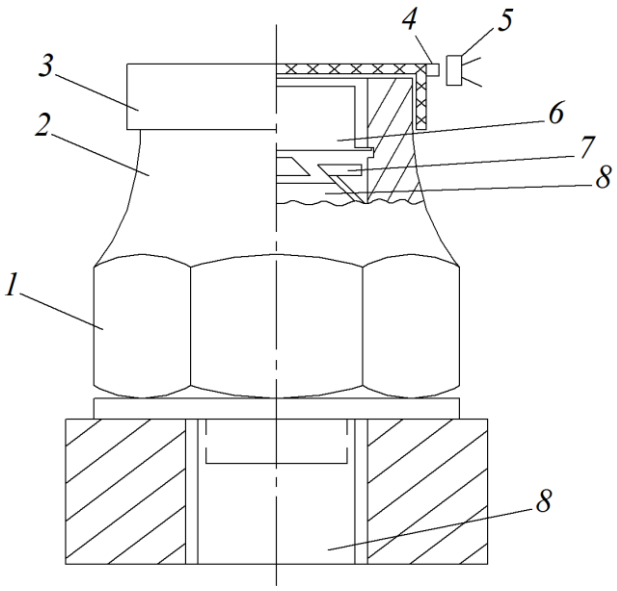

Figure 6. Nut-indicator for overheating of sectional casing of technological machine in assembled state

Here: 1 – nut, 2 – shank of a nut, 3 – protective cap, 4 – magnet, 5 – reed switch, 6 – rectangular signal flag, the outer surface of which has a bright fluorescing coating, 7 – thermosensitive element made of SME material in the form of a round unlatched washer, 8 – bolt.

Analysis of design and operation of thermal drives

Thermal drives with a power element based on SMA have significant advantages: less mass, they can work in a wide range of temperatures, small dimensions, smooth movement of working elements, lower cost. For example, the speed of the thermal-electric drive actuator increases due to the fixing device, which holds the leading element after heating and releases it to perform the working stroke under the influence of elastic deformation.

On Figure 7 a drive that is structurally manufactured as a single unit with a pump is shown.

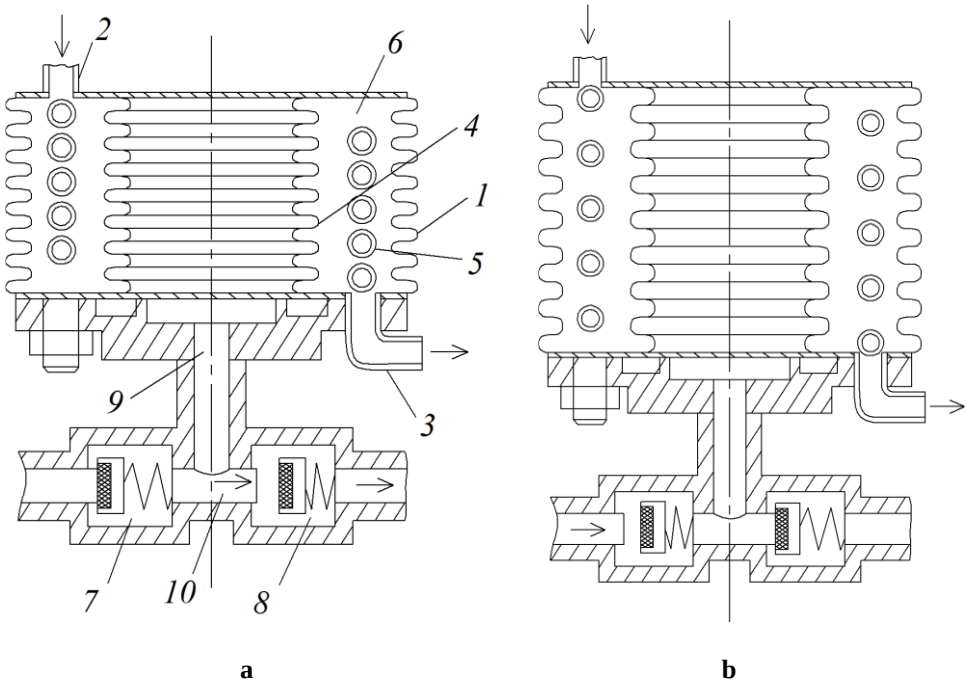

Figure 7. Pump
a – fluid suction mode; b – fluid discharge mode;
1 – bellows, 2,3 – pipes, 4 – piston, 5 – spring, 6 – round cavity, 7, 8 – valves,
9 – channel, 10 – cavity between valves.

The pump consists of a housing made as bellows 1 with pipes 2,3 for supply and release of heat transfer fluid, a piston that is also made in the form of bellows 4, a spring 5 that is made of SME material and a round cavity 6 between bellows 1 and 4.

When warm water (gas) is transfered to the heat-sensitive spring 5 through the pipe 2, the spring is heated to the starting point of reverse martensitic transformation. The length of the spring increases, and the bellows 1 and 4 straighten up. Fluid is sucked through the valve 7 to the cavity 10, the channel 9 and the bellows 4. At the end of the suction process, the supply of hot fluid is stopped and cold water (gas) is supplied to the spring 5. In this case there is direct martensitic transformation. The material of the spring rapidly changes its shape due to the anomalous change in its elasticity and plasticity. In this case, the spring shrinks, and the bellows 1 and 4 are compressed under the action of atmospheric pressure, fluid pushes out through the valve 8. Thereby, the pump operation is carried out by direct conversion of thermal energy into mechanical energy [2].

Work that is performed by the power element of the pump:

$$W = \sigma V \ln(1 + \varepsilon), \tag{7}$$

or

$$W = \Delta Q \frac{\Delta T_0}{T_0} \frac{\ln(1+\varepsilon)}{\varepsilon}, \tag{8}$$

where Ϭ – power that is generated by the SME material during its shape restoration, V,Ɛ – volume and relative linear deformation of the power element, respectively,
ΔQ – hidden heat of martensitic transformation, T_0, ΔT_0 – temperature of the thermodynamic equilibrium and its dislocation, caused by an external load, respectively.

The amount of heat that needs to be transferred to the working element to perform the mechanical work W:

$$Q \approx m(\Delta Q + \int_{M_f}^{A_s} C_p dT + \int_{A_s}^{A_f} C_p dT) \approx m(\Delta Q + C_p \Delta T_0) \quad (9)$$

where m – mass of the power element, C_p – heat capacity of the SME material, A_s, A_f, M_f – temperatures of the beginning and the end of reverse martensitic transformation and the temperature of the end of direct martensitic transformation, respectively.

W means maximum possible work. For nitinol alloy it is: $2 \cdot 10^4$ kJ/m^3.

Efficiency of the power element:

$$\eta = \frac{\ln(1+\varepsilon)}{\varepsilon} \frac{1}{T_0} \frac{1}{\frac{1}{\Delta T_0} + \frac{C_p}{\Delta Q}} \quad (10)$$

Analysis of design and operation of heliodrive

Construction of the heliodrive is shown on the Figure 8.

The main element of the drive is a heat-sensitive power element 1 made of SME material. Lens 6 is used as a sun-ray concentrator. A spring 5 returns the power element 1 to the initial position.

When sun rays hit the heat-sensitive element 1, it heats up to the starting point of reverse martensitic transformation. The shape of the element 1 is changed (Figure 8c) and it forces the rod 4 to move, compressing the spring 5. Joint nodes 2, 3 of the power element 1 allow the element to be moved at a certain distance and it falls into shadow. The heat-sensitive element is cooled over a certain period of time. This causes direct martensitic transformation. The material of the power element loses its original shape due to the rapid change in elasticity and plasticity. Under the action of the spring 5, the power element returns to its initial position. The drive is ready to work again. The frequency of operation cycles depends on the conditions of heating and cooling of the power element.

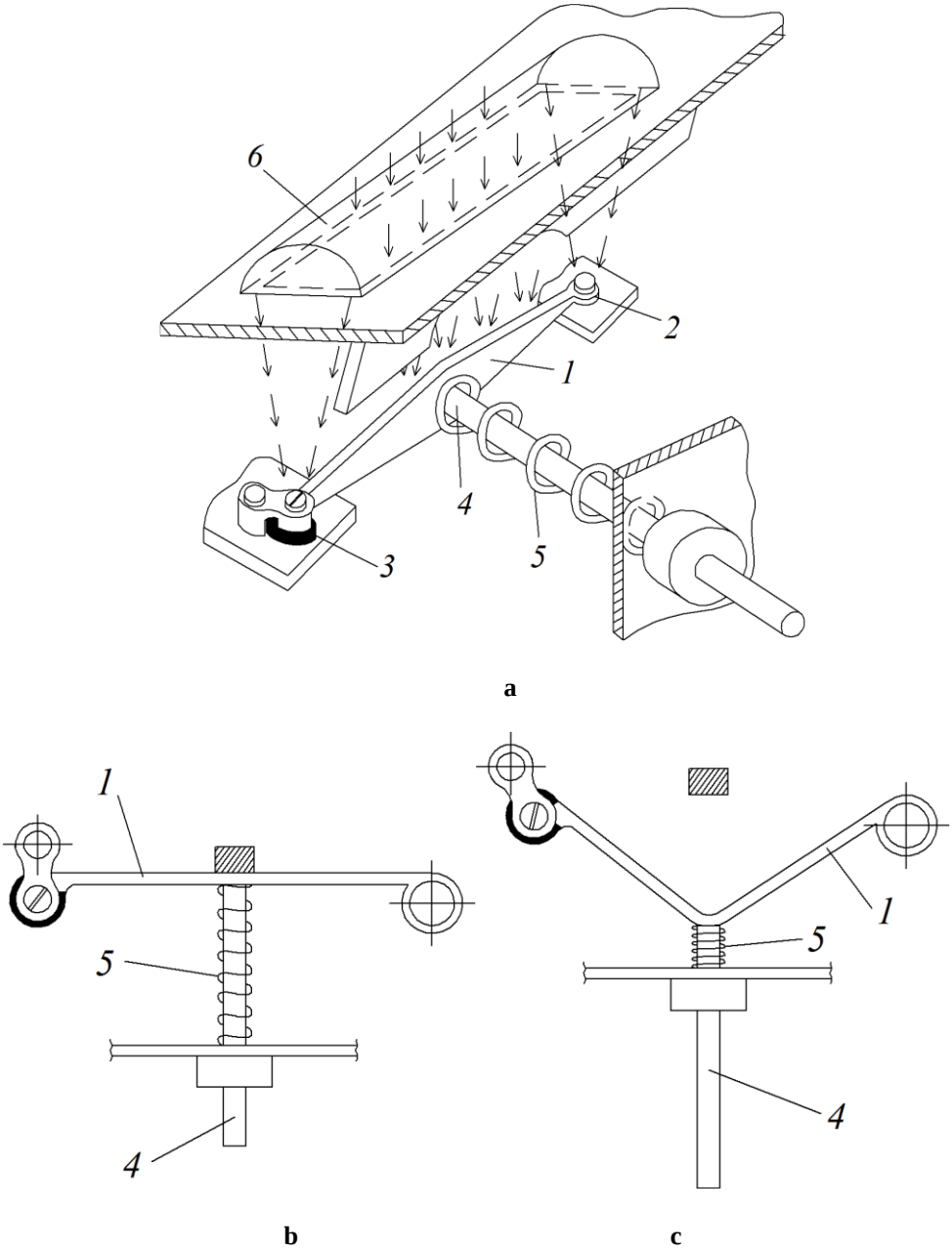

Figure 8. Heliodrive:
a – general view; b – power section in its initial state; c – power section after triggering; 1 – power element made from SME material; 2,3 – joint nodes for power element; 4 – rod; 5 – spring; 6 – lens.

Conclusions

1. The construction of the critical temperature increase indicator for machine's casing is marked by high manufacturability and reliability. The indicator does not lose its properties even when a machine is damaged. High corrosion resistance of nitinol ensures a service life of 30 years. Requirements of the heat-sensitive material are insignificant – one indicator needs several grams of the material. That's why additional costs can be paid off in one year
2. At many factories there is a need to utilize heat energy with a relatively small temperature difference. These requirements correspond to the design of the heat pump. The stable operation of this pump will be at a temperature difference in the range of 20...30°C, which is practically not realized in other known thermodynamic cycles. The temperature control can be carried out by any heat transferring fluid.
3. Power elements based on SME alloys have significant advantages: less mass, they can work in a wide range of temperatures, small dimensions, smooth movement of working elements, lower cost
4. Heat-sensitive elements with SME in the range of operating temperatures 290–320 °K have increased sensitivity in 200...400 times, comparatively to traditional materials.
5. Drives based on heat-sensitive elements with SME are effective in solar power plants.

References

1. Shesterenko V., Shesterenko O. (2017), *Proectuvannya system elektropostachannia*, PP "K", Kyiv.
2. Shesterenko V.Ye. (2011), *Systemy elektrospozhyvannia ta elektropostachannia promyslovykh pidpryiemstv*, Nova knyha, Vinnytsia.
3. Shesterenko V.Ye. (2001), *Optymizatsiia system elektrospozhyvannia promyslovykh pidpryiemstv*, Hlana, Kyiv.
4. Miková Ľ., Medvecká-Beňová S., Kelemen M., Trebuňa F., Virgala I. (2015), Application of shape memory alloy SMA as actuator, *Metalurgija*, 541, pp. 169–172.
5. Letenkov O.V., Filippov D.A. (2016), Calculation of the system drive: spring from material with shape memory effect – counter spring, *International research journal*, 11(53) Chapter 4, pp. 77–81.
6. Manikandan N., Kanchana J., Siva Sankar M., Radhakrishnan P. (2013), Design of Shape Memory Alloy Spring Actuator for Pinch Valve Actuation, *International Journal of Engineering Research & Technology*, 12(2), pp. 3089–3099.
7. Spaggiari A., Dragoni E. (2011), Multiphysics Modeling and Design of Shape Memory Alloy Wave Springs as Linear Actuators, *Journal of Mechanical Design*, 133(6), 061008.
8. Koh J.S. (2018), Design of Shape Memory Alloy Coil Spring Actuator for Improving Performance in Cyclic Actuation, *Materials (Basel, Switzerland)*, 11(11), 2324.
9. Liang C., Rogers C.A. (1993), Design of Shape Memory Alloy Springs With Applications in Vibration Control, *Journal of Vibration and Acoustics*, 115(1), pp. 129–135.
10. (2018), *Shape-memory alloys linear actuators: A new option for positioning*, Available at: https://www.designworldonline.com/shape-memory-alloys-linear-actuators-a-new-option-for-positioning

11. Benafan O., Brown J., Calkins T., Kumar P., Stebner A., Turner T., Vaidyanathan R., Webster J., Young M. (2014), Shape memory alloy actuator design: CASMART collaborative best practices and case studies, *International Journal of Mechanics and Materials in Design*, 10(1), pp. 1–42.
12. Leary M., Huang S., Ataalla T., Baxter A., Subic A. (2013), Design of shape memory alloy actuators for direct power by an automotive battery, *Materials & Design*, 43, pp.460–466.
13. Kalmar M., Boese A., Maldonado I., Landes R., Friebe M. (2019), NITINOL-based actuator for device control even in high-field MRI environment, *Medical Devices: Evidence and Research*, 12, pp. 285–296.
14. (1984), The Use of Shape Memory Alloys in Switchgear Technology, Available at: https://confluentmedical.com/wp-content/uploads/references/104.pdf
15. (2014), Green Relay Mechanisms Using Shape Memory Alloys, Available at: https://www.academia.edu/8371660/Green_Relay_Mechanisms_Using_Shape_Memory_Alloys
16. Barvinok V.A., Bogdanovich V.I., Lomovskoy O.V., Vishnyakov M.A., Groshev A.A. (2011), Razrabotka reversivnyih silovyih privodov iz materialov s effektom pamyati formyi dlya ustroystv, primenyaemyih v uzlah raschekovki kosmicheskih apparatov, *Izvestiya Samarskogo nauchnogo tsentra RAN*, 13(4), pp. 301.
17. Barvinok V.A., Bogdanovich V.I., Feokt V.S., Lomovskoy O.V. (1987), Malogabaritnoe oborudovanie i instrument s silovyim privodom iz splava s pamyatyu formyi, prednaznachennyie dlya vyipolneniya remontno-montazhnyih rabot, *Problemyi kosmicheskoy tehnologii metallov. Trudyi IES im.Patona*, pp. 99–103.
18. (2020), Hooke's law, Available at: https://en.wikipedia.org/wiki/Hooke%27s_law
19. Otsuka K., Wayman C.M. (1999), *Shape Memory Materials*, Cambridge University Press, Cambridge.
20. Duerig T.W., Pelton A.R. (1994), Ti-Ni shape memory alloys, *Materials Properties Handbook: Titanium Alloys*, American Society for Metals. pp. 1035–1048.
21. Oocuka K., Simidzu K., Sudzuki Yu. (1990), Splavy s effektom pamyati formy. Metallurgiya, Moscow.